Prediction of settlement trough induced by tunneling in cohesive ground

Mohammed Y. Fattah, Kais T. Shlash & Nahla M. Salim

Acta Geotechnica

ISSN 1861-1125

Acta Geotech.
DOI 10.1007/s11440-012-0169-4

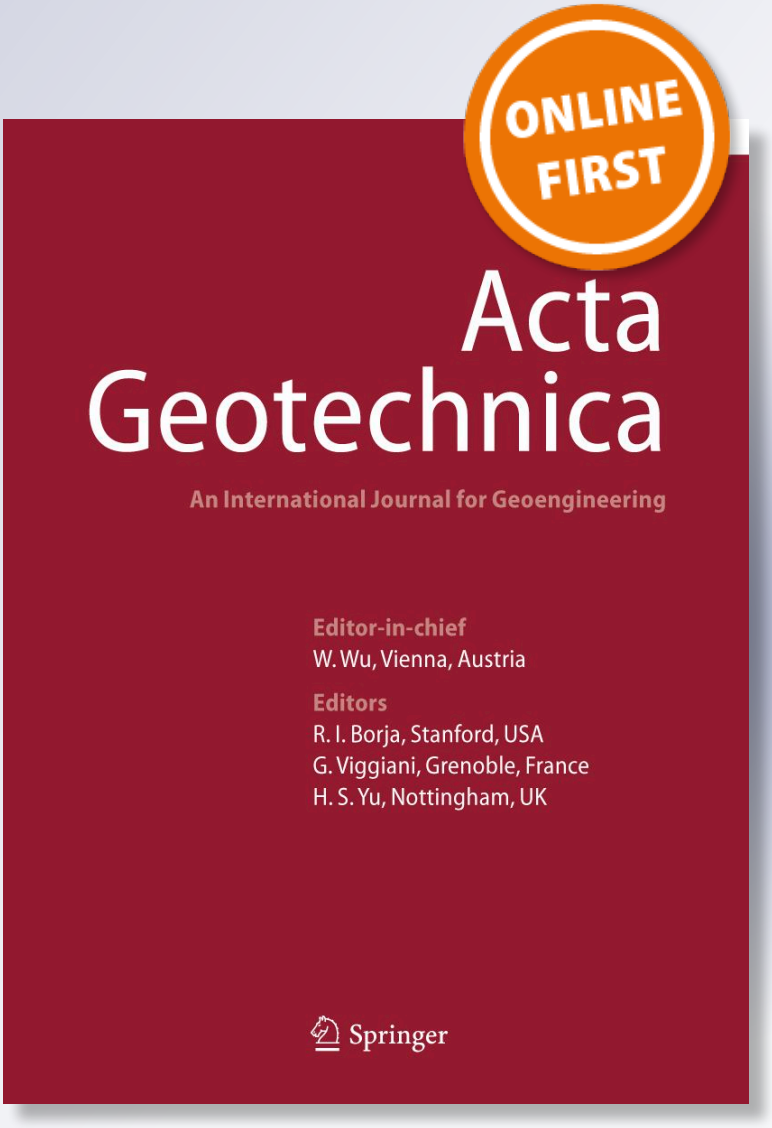

Springer

Acta Geotechnica
DOI 10.1007/s11440-012-0169-4

RESEARCH PAPER

Prediction of settlement trough induced by tunneling in cohesive ground

Mohammed Y. Fattah · Kais T. Shlash · Nahla M. Salim

Received: 2 November 2010 / Accepted: 5 April 2012

Abstract Surface settlements of soil due to tunneling are caused by stress relief and subsidence due to movement of support by excavation. There are significant discrepancies between empirical solutions to predict surface settlement trough because of different interpretations and database collection by different authors. In this paper, the shape of settlement trough caused by tunneling in cohesive ground is investigated by different approaches, namely analytical solutions, empirical solutions, and numerical solutions by the finite element method. The width of settlement trough was obtained by the finite element method through establishing the change in the slope of the computed settlement profile. The finite element elastic-plastic analysis gives better predictions than the linear elastic model with satisfactory estimate for the displacement magnitude and slightly overestimated width of the surface settlement trough. The finite element method overpredicted the settlement trough width i compared with the results of Peck for soft and stiff clay, but there is an excellent agreement with Rankin's estimation. The results show that there is a good agreement between the complex variable analysis for $Z/D = 1.5$, while using $Z/D = 2$ and 3, the curve diverges in the region faraway from the center of the tunnel.

Keywords Analytical solution · Clay · Finite elements · Settlement · Tunnel

M. Y. Fattah (✉) · K. T. Shlash · N. M. Salim
Building and Construction Engineering Department,
University of Technology, Baghdad, Iraq
e-mail: myf_1968@yahoo.com

1 Introduction

The construction of tunnel usually leads to some surface settlement. Often this settlement is of little importance to green field sites (i.e., those without surface structures), but may cause significant damage where surface structures are present.

Continuous research and advancement in tunnel technology lead to safer and both economically and environmentally efficient construction process. Beside obtaining field data to formulate empirical relationships of ground deformation, a major difficulty is the inconsistency of soil condition and applicability of the empirical formulas to different types of soil.

The available analytical solutions are not sufficient to include complex ground conditions, and hence, a comprehensive analytical solution coupled with numerical modeling is necessary to model the surface settlement.

Addenbrooke et al. [1] compared the plane strain predictions of ground movement for both single- and twin-tunnel excavations in stiff clay modeled as isotropic linear elastic-perfectly plastic, anisotropic linear elastic perfectly plastic, isotropic nonlinear elastic perfectly plastic with shear stiffness dependent on deviatoric strain and mean effective stress, and bulk modulus dependent on volumetric strain and mean effective stress, anisotropic non-linear elastic perfectly plastic employing the model above, and isotropic non-linear elastic perfectly plastic with shear and bulk stiffness dependent on deviatoric strain level, mean effective stress, and loading reversals. By considering the predicted surface settlement, the study carried out by Addenbrooke et al. [1] showed the importance of modelling non-linear elasticity, and the effect of introducing a soil independent shear modulus. The differences in subsurface displacements for isotropic and anisotropic models

Published online: 10 August 2012

were highlighted. The subsequent modeling of an adjacent tunnel excavation exposes more detailed features of all the models. It was concluded that anisotropic parameters appropriate to London Clay do not enhance the plane strain predictions of ground movement as long as nonlinear pre-failure deformation behavior is being modeled. A soft anisotropic shear modulus significantly improves green-field predictions but not twin-tunnel predictions and that accounting for load reversal effects does influence an analysis of the problem.

For initial stress regimes with a high coefficient of lateral earth pressure at rest, K_0, it has been shown by several studies that the transverse settlement trough predicted by (2D) finite element analysis is too wide when compared with field data. It has been suggested that 3D effects and/or soil anisotropy could account for this discrepancy. Franzius et al. [10] presented a suite of both 2D and 3D FE analyses of tunnel construction in London Clay. Both isotropic and anisotropic nonlinear elastic pre-yield models were employed, and it was shown that, even for a high degree of soil anisotropy, the transverse settlement trough remains too shallow. By comparing longitudinal settlement profiles obtained from 3D analyses with field data, it was demonstrated that the longitudinal trough extends too far in the longitudinal direction, and that consequently, it was difficult to establish steady-state settlement conditions behind the tunnel face. Steady-state conditions were achieved only when applying an unrealistically high degree of anisotropy combined with a low-K_0 regime, leading to an unrealistically high volume loss.

Masin [14] studied the accuracy of the three-dimensional finite element predictions of displacement field induced by tunneling using new Austrian tunneling method (NATM) in stiff clays with high K_0 conditions. The studies were applied to the Heathrow express trial tunnel. Two different constitutive models were used to represent London Clay, namely a hypoplastic model for clays and the modified cam-clay (MCC) model. Quality laboratory data were used for parameter calibration and accurate field measurements were used to initialize K_0 and void ratio. The hypoplastic model gave better predictions than the MCC model with satisfactory estimate for the displacement magnitude and slightly overestimated width of the surface settlement trough. Parametric studies demonstrated the influence of variation of the predicted soil behavior in the very-small-strain to large-strain range and the influence of the time dependency of the shotcrete lining behavior.

This paper discusses different approaches in predicting the settlement. The problem of settlement prediction is revisited, as was done by Chow [7]. In addition, this paper deals with analytical methods for tunnels in soft ground.

2 Characteristics of soft ground

Soft ground may consist of cohesive or cohesionless material. Sites used as case histories are frequently classified as one of these two types, although in reality, no site ever fits definition exactly. Previous researchers have recognized a difference in ground movements due to tunneling in two types of materials, with movements in cohesionless ground appearing to be restricted to a narrower region above the tunnel than in cohesive soils.

3 Surface settlement

There are two main causes for surface movements of soil due to tunneling:

- Stress relief: The stress relief mechanism causes an upward movement of soil. This is because, when soil is removed from the ground, there is a reduction in soil weight.
- Subsidence due to the removal of support during excavation: This causes a downward movement due to lack of support after the excavation.

Several researchers have studied the patterns of settlement trough by using one of the following four approaches:

1. Analytical solutions that include:
   (a) Elasticity solution,
   (b) Sagaseta's solution [22],
   (c) Modified analytical solution [25].
2. Empirical formulas.
3. Numerical solutions.
4. Physical modeling approaches.

These four approaches have their advantages and limitations.

4 Analytical solutions

4.1 Elasticity solution

Analytical solution exists for a point load acting beneath the surface of an infinite elastic half space [20], as in Mindlin's problem No. 1.

Chow [7] used this solution to estimate the settlement due to shallow tunneling, the effect of the tunnel face is ignored, and the tunnel is assumed to have infinite length. The unloading of the soil mass due to excavation is modeled as a line load along the tunnel axis. It is not possible to obtain analytically the integral of the point load solution (i.e., the solution for a line load), so relative differences in

vertical displacement are derived, which cancel the insoluble part of the integral. The surface settlement over the tunnel δ is then calculated as the settlement relative to some distance point on the surface, where the settlement is negligible [4].

$$\delta_z = -\frac{\gamma D^2 z^2}{8G(x^2+z^2)} \tag{1}$$

where D is the tunnel diameter, γ is the unit weight of soil, G is the shear modulus of soil, x is the horizontal distance from tunnel center, and z is the depth measured from tunnel center.

4.2 Sagaseta's method

For problems where only displacement boundary conditions are specified and when only displacements are required for the solution, Sagaseta [22] suggested to eliminate the stresses from the governing equations and work in terms of strain for simple soil models. An example of this problem is the determination of the displacement field in an isotropic homogeneous incompressible soil when some material is extracted at shallow depth, and the surrounding soil completely fills the void left by the extraction. Shallow tunneling in elastic homogeneous soil can be regarded as this type of problem, where the extracted material is defined by ground loss.

The advantage of Sagaseta's method is that the strain field obtained is independent of soil stiffness and is valid for incompressible material even for fluid. Sagaseta showed that closed-form solution for soil deformed due to ground loss (such as in tunnel excavation) can be obtained. Chow [7] used this approach to derive the solution for vertical displacement at the surface as:

$$\delta_z = -\frac{\gamma D^2 z^2}{4G(x^2+z^2)}. \tag{2}$$

The theoretical solutions provided by Sagaseta [22], which other authors modified to predict soft ground deformations due to tunneling, are essentially based on incompressible soils. Hence, it might not accurately predict the deformations in soft ground. Elastic solutions are more applicable for hard rock conditions.

Verruijt [24] reported that certain problems of stresses and deformations caused by deformation of tunnel in an elastic half plane can be solved by the complex variable method, as described by Muskhclishvili [15].

4.3 Complex variable solution

Verruijt and Booker [25] modified the analytical solutions for surface settlement using complex variable method. They considered Mindlin's problem of circular cavity in an elastic half plane loaded by gravity. The characteristics of this problem are that the stresses and strains due to the removal of the material inside a circular cavity are to be determined, with the stresses at infinity being determined by the action of gravity. This problem was solved by using complex variable method, with a conformal mapping of the region in the z plane.

5 Statement of Mindlin's problem

The problem will first be defined by giving all the relevant equations and the boundary conditions. The problem is solved by superposition of the three partial solutions. These solutions are as follows:

The first partial solution represents the stresses due to gravity in the half plane $z < 0$, without the cavity. This is a simple elementary solution.

$$\left.\begin{aligned} \sigma_z &= \gamma \cdot z \\ \sigma_x &= k_0 \cdot \gamma \cdot z \\ \tau_{xz} &= 0 \end{aligned}\right\} \tag{3}$$

In Mindlin's paper in 1910, only the values $k_0 = 0$, $k_0 = 1$, and $k_0 = \nu/(1-\nu)$ are considered, in which ν is Poisson's ratio. Verruijt and Booker [26] used the coefficient k_0 as an independent parameter determined by the geological history. The surface tractions along the cavity boundary can be related to the stresses. So the surface tractions in this case are found to be:

$$\left.\begin{aligned} t_x &= -K_0 \gamma z \sin\beta \\ t_z &= -\gamma z \cos\beta \end{aligned}\right\}. \tag{4}$$

The solution requires the representation of a function F, representing the integrated surface tractions along the cavity boundary in the form of a Fourier series, with the periodic parameters θ being the angular coordinate along the inner boundary CDC in the ξ-plane. This function F is related to the complex stress functions ϕ (y) and φ (ψ) by Verruijt and Booker [26]:

$$F = i\int_0^x (t_x + it_y)\mathrm{d}s = \varphi(y) + \overline{z\varphi'(y)} + \overline{\psi(y)} \tag{5}$$

where C is an arbitrary integration constant. The solution is detailed in (Appendix).

The complete solution of the problem consists of the sum of the three partial solutions. In order to verify the consistency and the accuracy of the solution, a computer program had been developed by Verruijt and Booker [26]. This program, named MINDLIN, enables the user to obtain numerical results of stresses and displacements in each point of the field, to construct different relationships and to validate the solution.

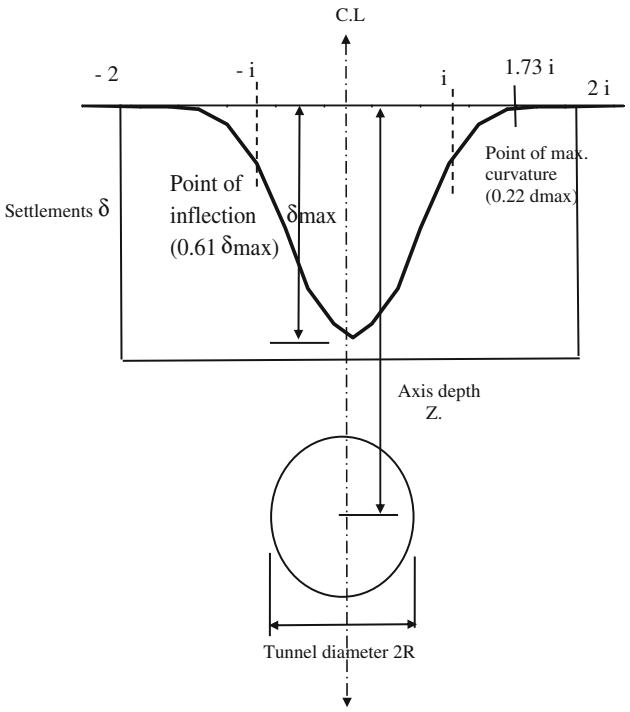

Fig. 1 Properties of error function curve to represent cross-section settlement trough above tunnel after [19]

6 Empirical solution

6.1 Empirical greenfield settlement trough

Peck [19] described settlement data from over twenty case histories. It follows that the short-term transverse settlement trough in the 'Greenfield' could be approximated by a normal distribution or Gaussian curve shown in Fig. 1. The equation representing the assumed trough shape is as follows:

$$\delta = \delta_{\max} \exp\left(-\frac{x^2}{2i^2}\right) \tag{6}$$

where δ is the surface settlement, $\delta_{\max}$ is the maximum vertical settlement, x is the transverse distance from tunnel centerline, and i is the width of settlement trough, which is the distance to the point of inflection of the curve (corresponding to one standard deviation of the normal distribution curve), and is determined by the ground conditions.

Various expressions have been proposed for calculating the trough width (i) as given in Table 1. In practice, the following relationship suggested by Rankin [21] is often used:

$$i = k \cdot Z_0 \tag{7}$$

where k is a dimensionless constant, depending on soil type: $k = 0.5$ for clay; $k = 0.25$ for cohesionless soils, Z_0 is the depth of the tunnel axis Z is shown in Fig. 1 below ground level.

Peck established a correlation between the relative depth of tunnel and the point of inflection of transverse surface settlement trough for various soil types.

Cording and Hansmire [9] and Peck [19] presented a normalized relation of the width parameter, $2i/D$, versus the tunnel depth, Z_0/D for tunnels driven through different geological conditions i.e.

$$\frac{2i}{D} = \left(\frac{Z_0}{D}\right)^{0.8} \tag{8}$$

in which D is the diameter of the tunnel.

Table 1 Different empirical solutions for estimation of settlement trough width, i

References	Width of settlement trough, i	Basis for empirical solution
Peck [19]	$i/R = (Z_0/2R)^n$ $(n = 0.8 - 1.0)$	Field observations
Attewell and Farmer [3]	$i/R = (Z_0/2R)^n$ $(a = 1.0, \quad n = 1.0)$	Field observations of UK tunnels
Atkinson and Potts [2]	$i = 0.25(Z_0 + R)$ (loose sand) $i = 0.25(1.5Z_0 + 0.5R)$ (dense sand and OC clay)	Field observations and model tests
Mair et al. [13]	$i = 0.5Z_0$	Field observations and centrifuge tests
Clough and Schmidt [8]	$i/R = (Z_0/2R)^n$ $(a = 1.0, \quad n = 0.8)$	Field observations of UK tunnels
O'Reilly and New [17]	$i = 0.43Z_0 + 1.1$ m cohesive soil $(3 \le Z_0 \le 35$ m) $i = 0.28Z_0 - 0.1$ m granular soil $(6 \le Z_0 \le 10$ m)	Field observations of UK tunnels
Leach (1986)[a]	$i = (0.57 + 0.55Z_0) \pm 1.01$ m	For sites where consolidation effects are insignificant
Rankin [21]	$i = k \cdot Z_0$ $k = 0.5$ for clay	Field observations

Z_0 tunnel depth

[a] Referred to by Chow [7]

Fujita [11] statistically analyzed the maximum surface settlement caused by shield tunneling based on 96 cases in Japan. A reasonable range of δ_{max} for different types of shield machines driven through different soil conditions with or without additional measures was suggested. A comparison of the various empirical methods discussed above was made on the assumption of a hypothetical four-meter-diameter tunnel located at a depth of thirty meters, which experience a ground volume loss of 1 % [23].

From comparison of various empirical solutions for surface settlement trough, the maximum settlement ranges from 3 to 5 mm, whereas the trough width i varies between 10 and 15 m. This shows that there are significant discrepancies between empirical solutions because of different interpretations and database collection by different authors (see Tan and Ranjith [23]).

7 Lateral movement

Lateral movements are studied more extensively than longitudinal movements. Norgrove et al. [16] derived an empirical equation that relates the subsurface settlement to the lateral deformations as shown below:

$$\frac{w_x}{w} = \frac{x}{c} \tag{9}$$

where w_x is the lateral deformation, w is the surface settlement at a distance x from the tunnel axis, c is the tunnel depth above the tunnel crown, and x is the horizontal distance from the tunnel axis.

O'Reilly and New [17] assumed that the resultant vectors of ground movements are directed to the tunnel axis and proposed an empirical equation similar to Norgrove et al. [16] with the vertical and horizontal components of the ground movements as δ_v and δ_h, and the horizontal surface settlement can be calculated as:

$$\delta_h = \left(\frac{x}{c}\right)\delta_v \tag{10}$$

where δ_v is the settlement at a distance x from the tunnel axis.

8 Analysis by the finite element method

The method of predicting the settlement trough is investigated, and the effect of rigid boundaries is explored. In using and developing a model, it is necessary to ensure that each technique used is correct, and they are mutually compatible. This is achieved by validation against existing solutions.

The problem studied by Chow [7] is reanalyzed in the following sections using the computer program Modf-CRISP.

9 Geometry of the problem and soil properties

The tunnel analyzed by Chow has a diameter of 5 m and different depths. The finite element mesh is shown in Fig. 2. The elements chosen in this application are six-node triangular and 8-node isoparametric quadrilateral elements for the two-dimensional plane strain problem. The material properties by Gunn [12] and representative of London clay as confirmed by Chow [7] are shown in Table 2.

The program Modf-CRISP provide different soil models, as follows:

1. Linear elastic.
2. Nonlinear elastic.
3. Elastic-perfectly plastic.

Oteo and Sagaseta [18] investigated the boundary effects in the finite element analysis of tunneling problem. It was found that the bottom rigid base has the most significant effect on the predicted settlements. When the depth of the rigid base below tunnel axis, H_D, increases, the settlements decrease, resulting in surface heave for a value of $H_D/D > 7$.

10 Computer program

CRISP allows elements to be removed to simulate excavation or added to simulate construction. Constitutive model with Mohr–Coulomb failure criterion is used (Britto and Gunn [5]).

When performing a nonlinear analysis involving excavation or construction, CRISP allows the effect of element removal or addition to be spread over several increments in an "incremental block." Element stiffness is always added or removed in the first increment of block, but the associated loads are distributed over all the increments in the block.

11 Linear elastic and elastic-plastic models

The analyses are divided into two categories: elastic and elastic-plastic. The analyses are carried out for:

- homogeneous soil.
- soil with properties varying with depth.

For each soil type, an analysis is made for three values of z, the depth below the surface of the tunnel axis. Values of z of 7.5, 10, and 15 m are used.

The first analysis is carried out for short-term movement, under undrained conditions, where the volumetric strain is zero. It follows that the value of undrained bulk modulus must be infinite, and Poisson's ratio equals 0.5. In finite element analysis, it is not possible to use an infinite

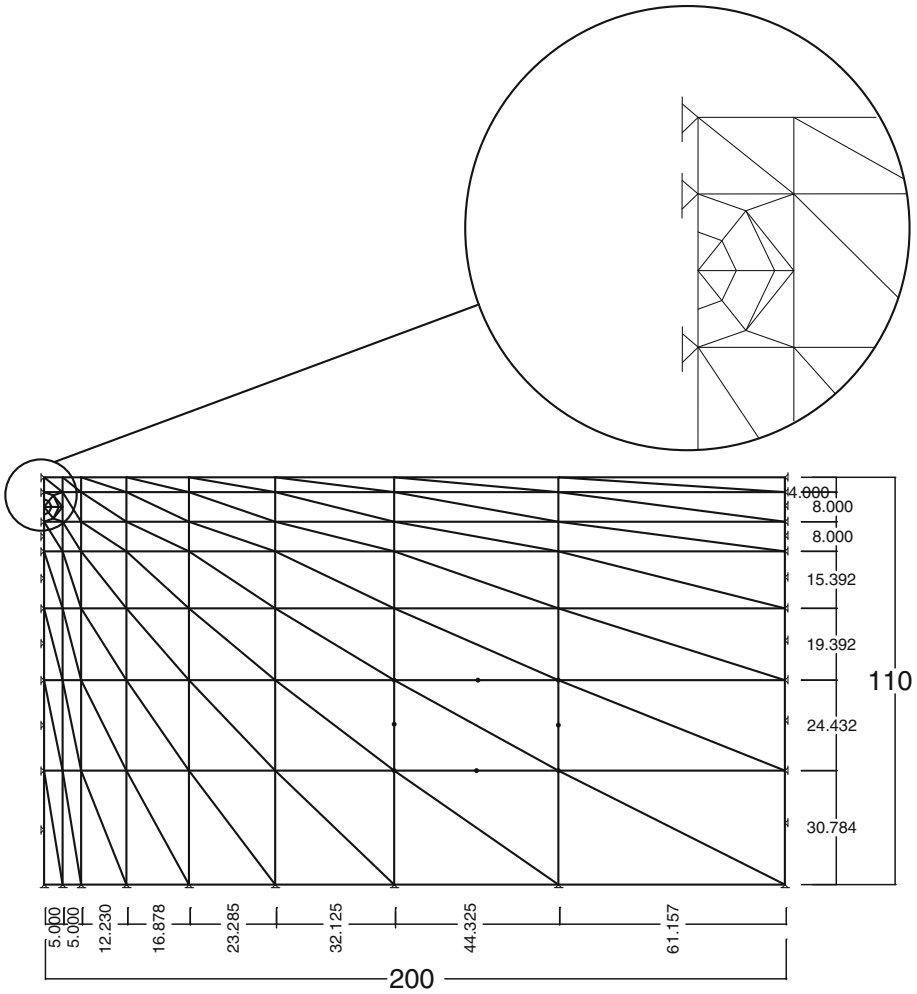

Fig. 2 The finite element mesh. All dimensions are in meters

Table 2 Soil properties for London clay [7]

Property	Value
Shear modulus, G (kPa)	33,500
Poisson's ratio, v	0.495
Unit weight of the soil, γ (kN/m^3)	20

undrained bulk modulus. To approximate undrained conditions, a value of Poisson's ratio of 0.495 is used. The following equation is used to represent the variation of soil stiffness with depth:

$$E = E_0 + m(z_0 - z) \tag{11}$$

where E is Young's modulus, E_0 is the initial Young's modulus at datum elevation, m is the rate of increase of Young's modulus with depth, z_0 is the depth of tunnel axis, and z is the depth to the point of interest.

So the shear modulus G will be forced to vary in the same way as E through the standard relationship $G = E/2(1 + v)$.

The value of G at a depth of 10 m is 33,500 kPa and is kept constant for all the analyses. The Mohr–Coulomb failure criterion is used to define the failure load for elastic-plastic model.

12 Mechanism of short-term settlement response

Analytical approaches often require the identification of non-dimensional group of the important parameters influencing a problem. One such group is the stability number (or overload factor). N is defined by Broms and Bennermark [6] as:

$$N = \frac{(\sigma_z - \sigma_T)}{S_u} \tag{12}$$

where σ_z is the overburden pressure at the tunnel axis, σ_T is the tunnel support pressure or internal pressure (if any), and S_u is the undrained shear strength of clay, if $\sigma_T = 0$, then N will be:

$N = \sigma_z/S_u = \gamma Z/S_u,$

where $Z = C + D/2$, C is the depth of tunnel crown.

Three values of $(S_u/\gamma{\cdot}z)$ are used in the present analyses. The values of $(S_u/\gamma{\cdot}z)$ and their corresponding S_u for each (Z/D) are given in Table 3.

In the present analysis, three values of $S_u/\gamma{\cdot}z$ for three depths of the tunnel axis are used. These values are presented in Tables 4 and 5. The analyses were carried out using homogeneous elastic analysis and homogeneous elastic perfectly plastic analysis.

13 Presentation of results

13.1 Linear elastic analysis

The results obtained of three different depths of the tunnel ($Z/D = 1.5$, 2 and 3) using the program Modf-CRISP are shown in Fig. 3 and presented in dimensionless form as $\delta G/\gamma D^2$ versus X/D. Heave is noticed for $Z/D = 1.5$, 2, and 3. This is because the movement of the soil is upward due to relief effect of excavated soil in a purely elastic homogeneous medium. As X/D increases, the upward movement of the soil decreases, this is because that the soil is remote from concentration of loading. These results conform to Chow [7] as illustrated in Fig. 4.

Figures 5, 6, and 7 show a comparison of the surface settlement predicted by different analytical methods. The results show that there is a good agreement between the complex variable analysis and the finite element for $Z/D = 1.5$, while using $Z/D = 2$ and 3, the curves diverge in the region far way from the center of the tunnel, but the behavior is similar to that of the curve using complex variable method. A good agreement with elastic and Sagaseta's solution is shown in the region far away from the center of the tunnel, while heave can be noticed in the region near the center of tunnel using the finite element analysis.

Table 3 Values of S_u used for different depths of tunnel analysis

$N = \frac{\sigma_z}{S_u} = \frac{\gamma z}{S_u}$	3.33			2.5			2.0		
$S_u/(\gamma{\cdot}z)$	0.3			0.4			0.5		
C/D	1.0	1.5	2.5	1.0	1.5	2.5	1.0	1.5	2.5
Z (m)	7.5	10	15	7.5	10	15	7.5	10	15
Z/D	1.5	2.0	3.0	1.5	2.0	3.0	1.5	2.0	3.0
S_u (kPa)	45	60	75	60	80	100	90	120	150

Table 4 Soil properties used for linear elastic model from [7]

	Homogeneous			Non homogenous		
Z (m)	7.5	10	15	7.5	10	15
Z/D	1.5	2.0	3.0	1.5	2.0	3.0
G_0 (kPa)	33,500	33,500	33,500	0	0	0
m (kPa/m)	0	0	0	3,350	3,350	3,350
Reference	1.5eh	2eh	3eh	1.5en	2en	3en

e elastic; *n* non homogeneous; *h* homogeneous

Table 5 Soil properties used for elastic, perfectly plastic homogeneous analysis from [7]

	Homogeneous								
Z (m)	7.5			10			15		
Z/D	1.5			2.0			3.0		
G_0 (kPa)	33,500			33,500			33,500		
m (kPa/m)	0			0			0		
S_{u0} (kPa)	45	60	90	60	80	100	90	120	150
$S_u/(\gamma{\cdot}z)$	0.3	0.4	0.5	0.3	0.4	0.5	0.3	0.4	0.5
References[a]	1.5 ph3	1.5 ph4	1.5 ph5	2 ph3	2 ph4	2 ph5	3 ph3	3 ph4	3 ph5

[a] $Z/D = 1.5$, 2 and 3

e, elastic; *n*, non homogeneous; *p,* plastic; *h,* homogeneous

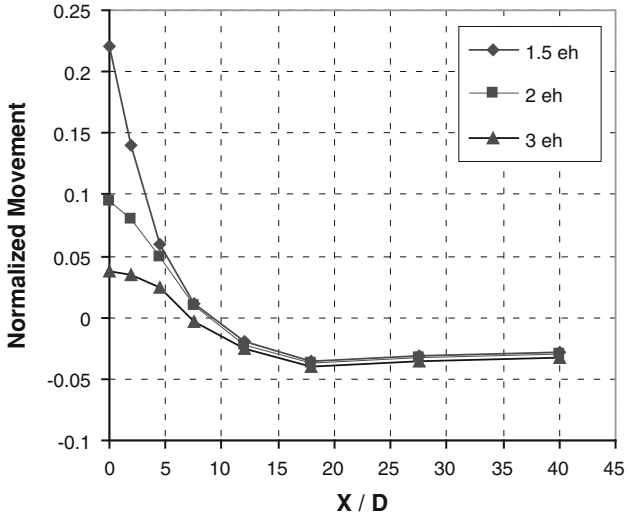

Fig. 3 Surface displacement for elastic homogeneous soil model predicted by the finite element method for different *Z*/*D* ratios. Normalized Movement = $\delta G/\gamma D^2$

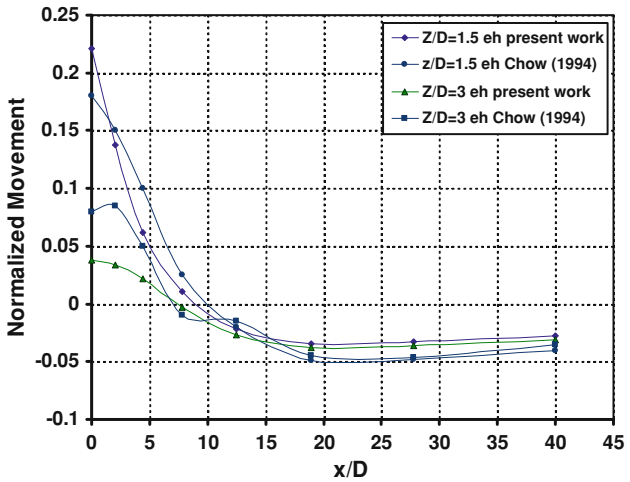

Fig. 4 Comparison of the analysis results with Chow's results for different *Z*/*D* ratios using elastic homogeneous model

Figures 8 and 9 show the variation of the surface horizontal movement using the complex variable analysis and the finite element analysis, respectively. It is clearly shown that the maximum horizontal movement tends to be toward the tunnel as *Z*/*D* decreases using the complex variable method while the maximum horizontal movement moves away from the center of the tunnel as *Z*/*D* decreases using the finite element method. The comparison between the two results is clearly shown in Figs. 10, 11, and 12 for different *Z*/*D* values.

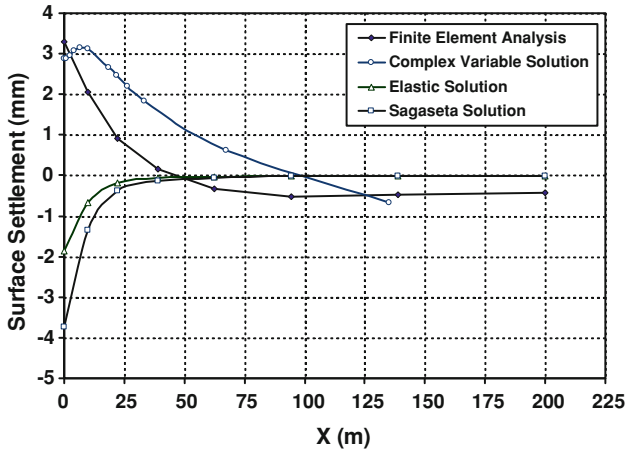

Fig. 5 Comparison between different approaches in predicting the surface settlement (*Z*/*D* = 1.5)

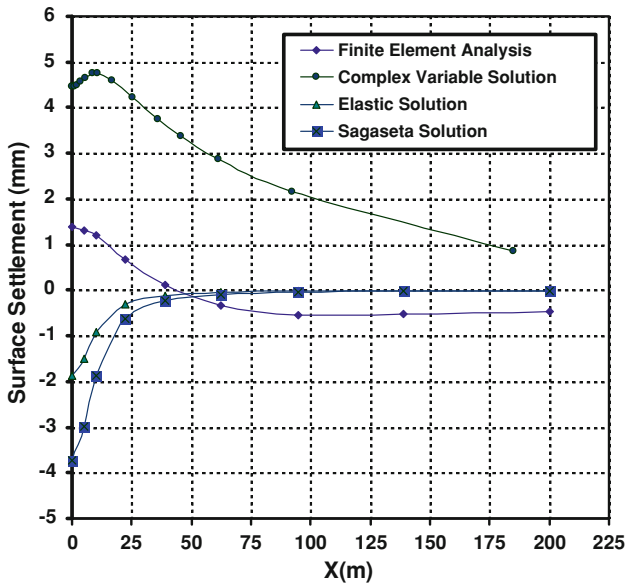

Fig. 6 Comparison between different approaches in predicting the surface settlement (*Z*/*D* = 2)

13.2 Elastic non-homogeneous soil model

CRISP provides a non-homogeneous model in which the material properties can vary with depth. This method is used in the present work, dimensionless plot of $\delta G/\gamma D^2$ against *X*/*D* is shown in Fig. 13. The results show that settlements are predicted for *Z*/*D* = 2 and 3 while heave can be noticed for *Z*/*D* = 1.5.

13.3 Elastic-plastic analysis

The dimensionless settlement profile obtained using elastic-plastic homogeneous soil is shown in Figs. 14, 15, and 16, each plot corresponds to a constant value of $S_u/\gamma \cdot z$.

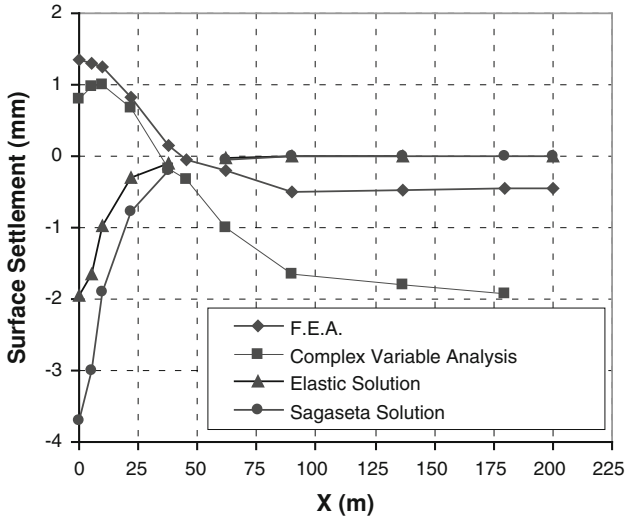

Fig. 7 Comparison between different approaches in predicting the surface settlement ($Z/D = 3$)

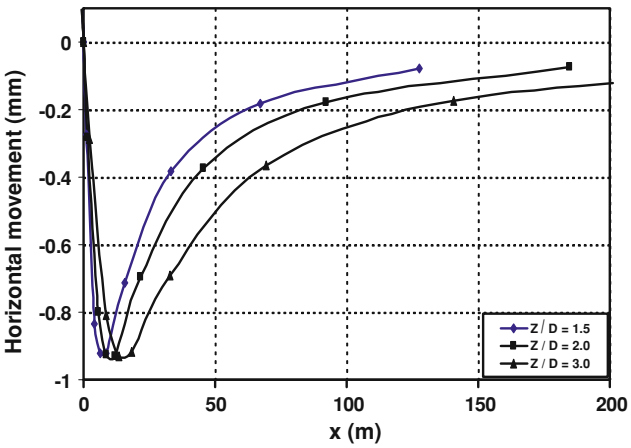

Fig. 8 Surface settlement using the complex variable analysis

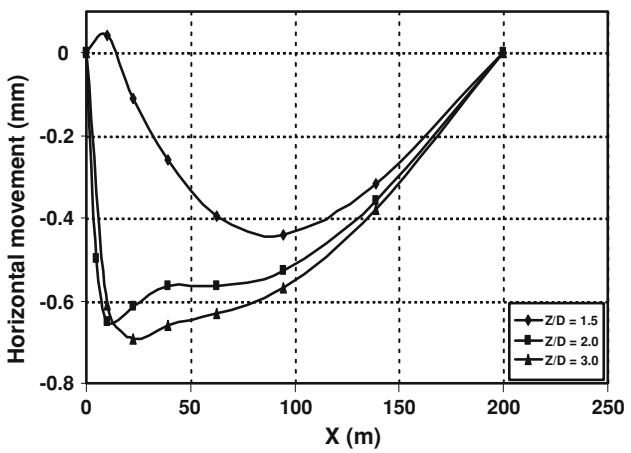

Fig. 9 Surface settlement using the finite element analysis

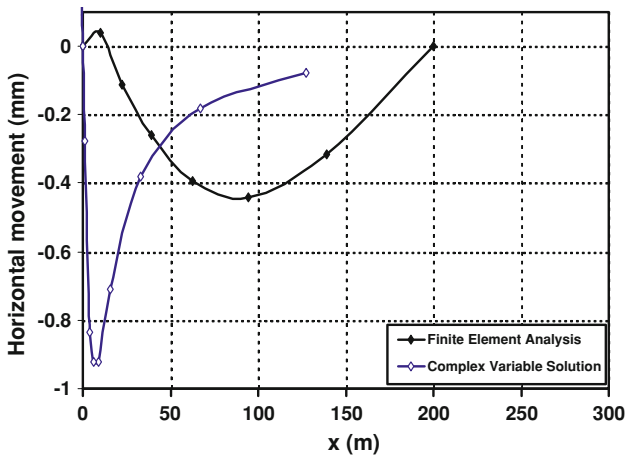

Fig. 10 Comparison of the surface settlement obtained by the finite element method with complex variable results ($Z/D = 1.5$)

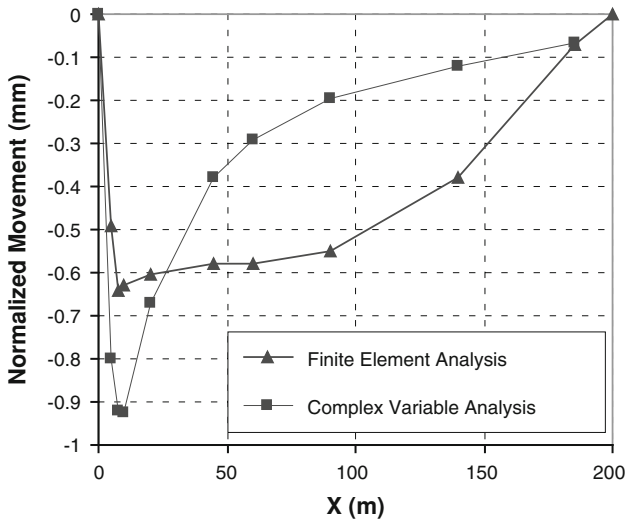

Fig. 11 Comparison of the surface settlement obtained by the finite element method with complex variable results ($Z/D = 2$)

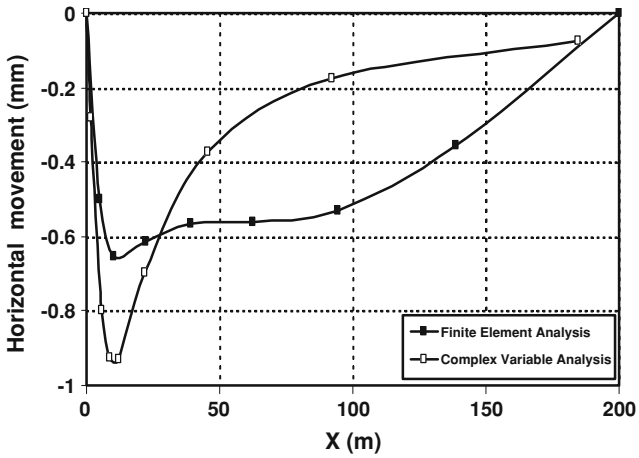

Fig. 12 Comparison of the surface settlement obtained by the finite element method with complex variable results ($Z/D = 3$)

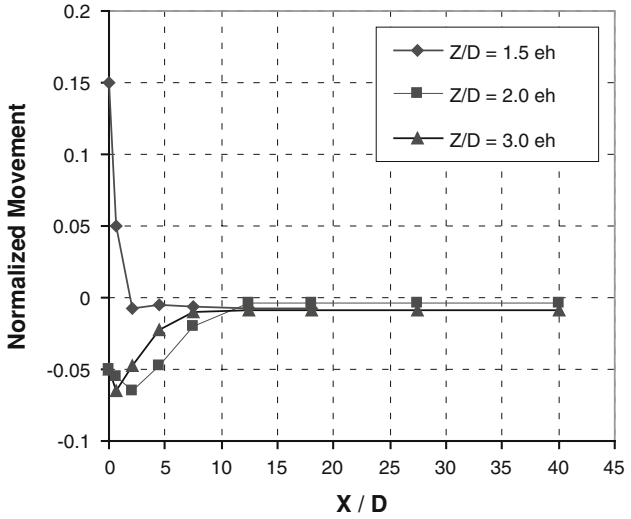

Fig. 13 Surface displacement predicted by the finite element method using elastic nonhomogeneous soil model for different *Z*/*D* ratios

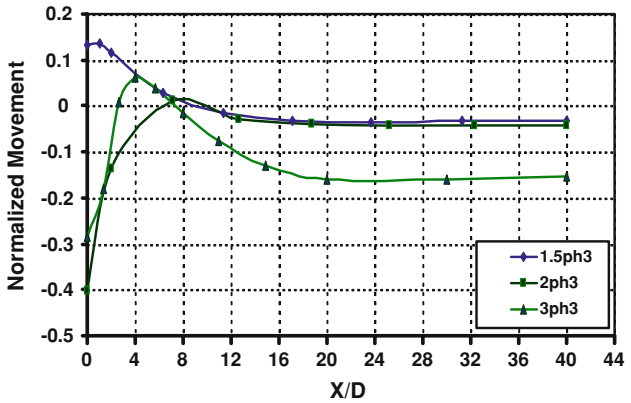

Fig. 14 Surface displacement using elastic-plastic homogeneous soil model predicted by the finite element method for different *Z*/*D* ratios and $S_u/\gamma{\cdot}z = 0.3$

Figure 14 shows that for $S_u/\gamma{\cdot}z = 0.3$, settlements are obtained above the tunnel for $Z/D = 2$ and 3 (2 ph3, 3 ph3), while heave can be obtained at $Z/D = 1.5$. Increasing $S_u/\gamma{\cdot}z$ to 0.4 causes heave when $Z/D = 2$ and 3, while settlement is noticed at $Z/D = 1.5$ as shown in Fig. 15. Further increase in $S_u/\gamma{\cdot}z$ to 0.5 causes heave to be obtained for three values of Z (1.5 ph5, 2 ph5, 3 ph5) as shown in Fig. 16.

13.4 Trough width parameter (i)

As explained previously, the trough width parameter i describes the width of settlement trough. To evaluate the width of the settlement trough, i, there are two methods:

1. Using linear regression to obtain the gradient of the plot of $\ln \delta/\delta_{max}$ versus X^2 for each settlement profile, and the value of the gradient is equal to $-1/(2i^2)$

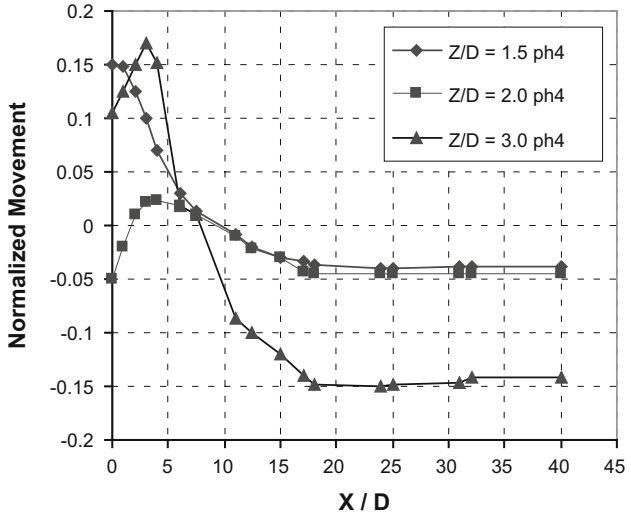

Fig. 15 Surface displacement using elastic-plastic homogeneous soil model predicted by the finite element method for different *Z*/*D* ratios and $S_u/\gamma{\cdot}z = 0.4$

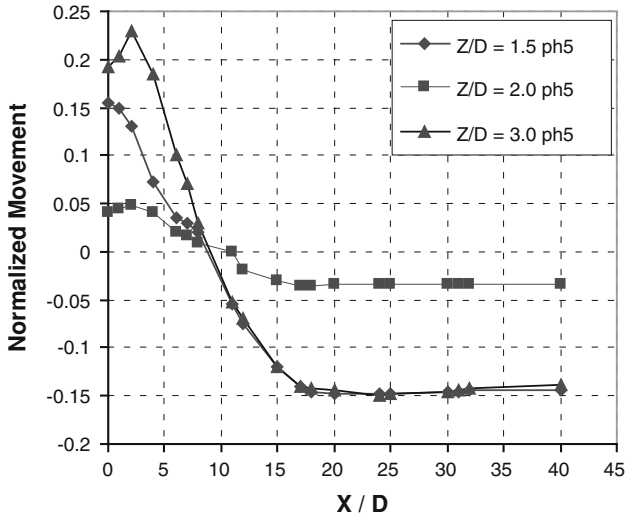

Fig. 16 Surface displacement using elastic-plastic homogeneous soil model predicted by the finite element method for different *Z*/*D* ratios and $S_u/\gamma{\cdot}z = 0.5$

2. Establishing the change in the slope of the computed settlement profile.

The first method assumes that the predicted settlement profiles follow the shape of an error function curve:

$$\delta = \delta_{max} \exp\left(-x^2/\left(2i^2\right)\right) \tag{13}$$

Taking natural log for the above equation gives

$$\ln \delta = \ln \delta_{max} - x^2/\left(2i^2\right). \tag{14}$$

By plotting $\ln \delta/\delta_{max}$ versus x^2, the gradient obtained would be equal to $-1/(2i^2)$, and the value of i can be

evaluated. The disadvantage of this method lies in the assumption made for the shape of the predicted settlement trough. Although field investigations carried out by Peck [19] showed that surface settlements in tunneling problems could fit with this type of probability function, computed settlements did not necessarily produce results that could be represented by this type of probability function. This is due to the fact that the data from field investigations were usually obtained in a region comparatively close to the tunnel (e.g., <20 m). The predicted value of i becomes inaccurate since it is obtained from the gradient of $\ln \delta/\delta_{max}$ versus x^2 plot and is taken as the best fit line for the total horizontal width of the finite element mesh (200 m in this case).

The second method was achieved by establishing the point where the change in the slope of the settlement profile from positive to negative occurs. Since the computed settlement profile was plotted by joining the vertical displacement of each node on the surface of the mesh using straight lines, therefore the change in the slope of the settlement profiles were represented by a change in the gradient. This method considers the whole range of x, and it is more reliable than the first method.

The second method was used and plots of i/D against Z/D are presented in Fig. 17. The results are obtained from Peck's field investigation for the values of i/D for the range of values for Z/D (1.5–3) for soft to stiff clays, and the results are also obtained using different equations to estimate the settlement trough width (i). The results reveal that the finite element analysis overpredicts the settlement trough width (i). This may be due to the plastic behavior of the soil.

Elastic analysis was carried out with $C/D > 3$ to represent a deep tunnel behavior with $\sigma_h = \sigma_v$ and $\gamma_{soil} = 20$ kN/m^3. The settlement trough obtained in the analysis is compared with different analyses explained early. A good agreement is obtained between the finite element analysis and elastic analysis.

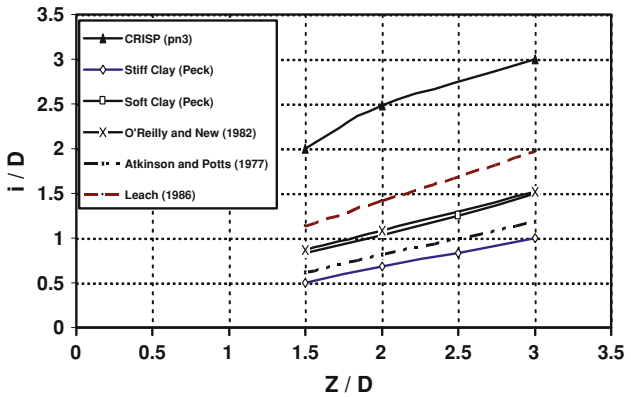

Fig. 17 Plot of i/D against Z/D using different methods in estimation of the settlement trough width (i)

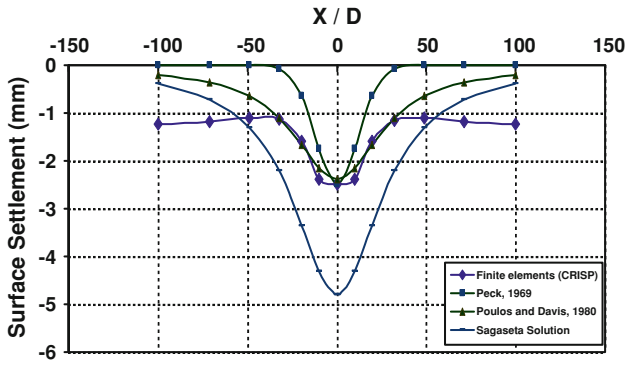

Fig. 18 Surface settlement obtained from different approaches (deep tunnel) $Z_0 = 30$ m, diameter $= 4$ m

Table 6 Estimation of the settlement trough width (i) using different approaches

Z (m)	D (m)	i (m)			
		Finite elements (present study)	Peck [19]	O'Reilly and New [17]	Rankin [21]
30	4	15	9.48	12.69	15

The surface settlement values calculated using different approaches are shown in Fig. 18. The conclusion drawn is that there is a good agreement between the finite element results and the elastic solution in the region near to the center of the tunnel, but the settlement trough is wider than Peck's solution and narrower than Sagaseta elastic solution.

The estimation of the settlement trough (i) for deep tunnel using different approaches is listed in Table 6.

The results show that there is a good agreement with [17, 21], but there is an approximately 36 % difference from Peck's estimation. This difference is due to the fact that Peck used the probability function in the estimation of ii which may not necessarily fit with the present results.

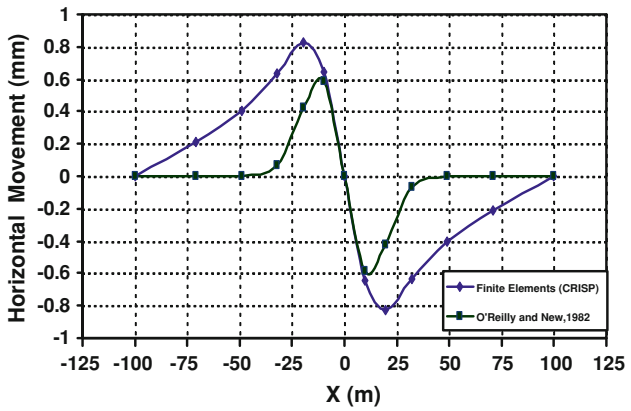

Fig. 19 Horizontal movement using different approaches for deep tunnel $Z_0 = 30$ m, diameter $= 4$ m

Figure 19 shows the horizontal surface displacement obtained from the finite element results and empirical (Gaussian) solution (Eq. 14). Here, the Gaussian model prediction is based on the assumption that the vectors of ground movement are oriented toward the tunnel axis [17]. For the tunnel model, both the form (allowing for the trough being too wide) and the magnitude of maximum movement are similar to the Gaussian model.

14 Conclusions

This paper focuses on the prediction of the surface settlement due to tunneling. The surface settlements were estimated using different methods, analytical, empirical, and the finite elements. The conclusions drawn from this analysis are as follows:

1. In elastic homogeneous medium, the upward movement of the soil is due to relief effect of the excavated soil above the tunnel, but this movement decreases as X/D increases. This is because the soil is remote from concentration of loading.
2. The results show that there is a good agreement between the complex variable analysis for $Z/D = 1.5$, while using $Z/D = 2$ and 3, the curve diverges in the region faraway from the center of the tunnel.
3. The finite element elastic-plastic analysis gave better predictions than the linear elastic model with satisfactory estimate for the displacement magnitude and slightly overestimated width of the surface settlement trough.
4. The finite element method overpredicted the settlement trough width i compared with the results of Peck for soft and stiff clay, but there is an excellent agreement with Rankin's estimation.
5. The maximum horizontal movement tends to be toward the tunnel as Z/D decreases using the complex variable method, while the maximum horizontal movement moves away from the center of the tunnel as Z/D decreases using the finite element method.

Appendix

Mindlin's problem

In the ξ-plane, the function F is to be considered along the boundary $\xi = \alpha\sigma = \alpha\exp(i\theta)$

$$F = i\int_0^s (t_x + it_z)\,\mathrm{d}s \tag{15}$$

where the integration path should be such that the material (inside the cavity) lies to the left when traveling along the integration path. This means that $\mathrm{d}s = -r\mathrm{d}\beta$. Because on the boundary of the cavity $z = -h - r\cos\beta$, it follows that the boundary function F for this part of the solution, which will be denoted by F_1, is:

$$\frac{F_1}{\gamma\cdot r} = -\int_0^\beta \left[h\cos\beta + r\cos^2\beta\right]\mathrm{d}\beta - ik_0\int_0^\beta \left[h\sin\beta = r\sin\beta\cos\beta\right]\mathrm{d}\beta. \tag{16}$$

Elaboration of the integrals gives

$$\frac{F_1}{\gamma\cdot r} = -\frac{1}{2}r\beta - \frac{1}{4}r\sin 2\beta - h\sin\beta - ik_0\left[h(1-\cos\beta) + \frac{1}{4}r(1-\cos 2\beta)\right] \tag{17}$$

The expression (17) gives the integrated surface traction F_1 as a function of β, the angular coordinate along the circular boundary in the z plane. This quantity is needed, however, as a function of θ, the angle along the inner circular boundary in the ξ-plane, for that reason the relation between these two angles:

$$\theta = w(\xi) = -ih\frac{1-\alpha^2}{1+\alpha^2}\frac{1+\xi}{1-\xi^2} \tag{18}$$

where α is the geometric parameter r/h, and the ratio of the radius of the circular cavity to its depth is as follows:

$$\frac{r}{h} = \frac{2\alpha}{1+\alpha^2} \tag{19}$$

Along the inner circular boundary in ξ-plane $\xi = \alpha\sigma = \alpha.\exp(i\theta)$, with equation (18) this gives, after some mathematical manipulations:

$$\frac{x}{r} = \frac{(1-\alpha^2)\sin\theta}{(1+\theta^2) - 2\alpha\cos\theta} \tag{20}$$

$$\frac{z+h}{r} = -\frac{(1+\alpha^2)\cos\theta - 2\alpha}{(1+\alpha^2) - 2\alpha\cos\theta} \tag{21}$$

These equations represent a circle of radius r around a point at a depth h, because:

$$x^2 + (z+h)^2 = r. \tag{22}$$

The angle β can be expressed as:

$$\tan\beta = \frac{x}{z+h} = \frac{(1-\alpha^2\sin\theta)}{(1+\alpha^2)\cos\theta - 2\alpha} \tag{23}$$

The value of β is defined such that it varies continuously from $\beta = 0$ to $\beta = 2\pi$ in the interval from $\theta = 0$ to

$\theta = 2\pi$. This can be accomplished by modifying the standard function l = arc tan (z/x) in such a way that for values of x and z in four quadrants, the value of the function varies continuously from 0 to 2π when $\theta = 0$ to $\theta = 2\pi$.

The function F_1 can be calculated from the formula (17), which can be written as:

$$\frac{F_1}{\gamma\pi r^2} = \frac{\beta}{2\pi} - \frac{\sin 2\pi}{4\pi} - \frac{1}{\pi}\frac{h}{r}\sin\beta - \frac{iK_0}{\pi}\left[\frac{h}{r}(1-\cos\beta) + \frac{1}{4}(1-\cos 2\beta)\right] \quad (24)$$

References

1. Addenbrooke T, Potts D, Puzrin A (1997) The influence of pre-failure soil stiffness on the numerical analysis of tunnel construction. Geotechnique 47(3):693–712
2. Atkinson JH, Potts DM (1977) Stability of a shallow circular tunnel in cohesionless soil. Geotechnique 27(2):203–213
3. Attewell PB, Farmer IW (1974) Ground deformation resulting from shield tunneling in London clay. Can Geotech J Can 11(3):380–395
4. Augard CE (1997) Numerical modeling of tunneling processes for assessment of damage to building. Ph.D. thesis, University of Oxford
5. Britto AM, Gunn MJ (1987) Critical state soil mechanics via finite elements. Wiley, New York
6. Broms BB, Bennermark H (1967) Stability of clay at vertical openings. J Soil Mech Found Div ASCE 93(SM1):71–95
7. Chow L (1994) Prediction of surface settlement due to tunneling in soft ground. MSc. thesis, University of Oxford
8. Clough GW, Schmidt B (1981) Excavation and tunneling. In: Brand EW, Brenner RP (eds) Soft clay engineering, Chap 8. Elsevier
9. Cording EJ, Hansmire WH (1975) Displacement around soft ground tunnels. General Report: Session IV, Tunnels in Soil. In: Proceedings of 5th Panamerican congress, on soil mechanics and foundation engineering
10. Franzius JN, Potts DM, Burland JB (2005) The influence of soil anisotropy and K_0 on ground surface movements resulting from tunnel excavation. Geotechnique 55(3):189–199
11. Fujita K (1982) Prediction of surface settlements caused by shield tunneling. In: Proceedings of the international conference on soil mechanics, vol 1. Mexico City, Mexico, pp. 239–246
12. Gunn M (1993) The prediction of surface settlement profiles due to tunneling. In: Predictive soil mechanics, proceedings of worth memory symposium. Thomas Telford, London, pp 304–316
13. Mair R, Gunn M, O'Reilly M (1981) Ground movements around shallow tunnels in soft clay. In: Proceedings of 10th international conference on soil mechanics and foundation engineering, vol 2, Stockholm, pp 323–328
14. Masin D (2009) 3D modeling of an NATM tunnel in high K_0 clay using two different constitutive models. J Geotech Geoenviron Eng ASCE 135(9):1326–1335
15. Muskhclishvili NI (1953) Some basic problem of the mathematical theory of elasticity (Translated from Russian by Radok Noordhoff JRM) Groniyer
16. Norgrove WB, Cooper I, Attewell PB (1979) Site investigation procedures adopted for the northumbrian water authority's tyne side sewerage scheme, with special reference to settlement prediction when tunneling through urban areas. In: Proceedings of Tunneling, vol 79, London, pp 79–104
17. O'Reilly MP, New BM (1982) Settlements above tunnels in the UK-their magnitude and prediction. Tunneling 82:173–181
18. Oteo CS, Sagaseta C (1982) Prediction of settlements due to underground openings. In: Proceedings of international symposium numerical method in geomechanics Zurich, Balema, pp 653–659
19. Peck RB (1969) Deep excavations and tunneling in soft ground. In: Proceedings of the 7th international conference on soil mechanics and foundation engineering, state of the art volume, Mexico pp 225–290
20. Poulos HG, Davis EH (1974) Elastic solutions for soil and rock mechanics. Wiley, New York
21. Rankin W (1988) Ground movements resulting from urban tunneling. In: Prediction and effects, proceedings of 23rd conference of the engineering group of the geological society, London Geological Society, pp 79–92
22. Sagaseta C (1987) Analysis of undrained soil deformation due to ground loss. Geotechnique 37(3):301–320
23. Tan WL, Ranjith PG (2003) Numerical analysis of pipe roof reinforcement in soft ground tunneling. In: Proceedings of the 16th international conference on engineering mechanics
24. Verruijt A (1997) A complex variable solution for deforming circular tunnels in an elastic half-plane. Int J Numer Anal Methods Geomech 21:77–89
25. Verruijt A, Booker JR (1996) Surface settlements due to deformation of a tunnel in an elastic half- plane. Geotechnique 46(4):753–756 (London, England)
26. Verruijt A, Booker JR (2000) Complex variable solution of Mindlin's problem of an excavated tunnel. In: Developments in theoretical geomechanics. A.A. Balkema, Rotterdam, pp 3–22